universe

MDPI

Review

Challenges of the Standard Cosmological Model

Eleonora Di Valentino

School of Mathematics and Statistics, University of Sheffield, Hounsfield Road, Sheffield S3 7RH, UK; e.divalentino@sheffield.ac.uk

Abstract: Measurements of the temperature and polarization anisotropy of the cosmic microwave background (CMB) provided strong confirmation of the vanilla flat ΛCDM model of structure formation. Even if this model fits incredibly well, the cosmological and astrophysical observations in a wide range of scales and epochs, some interesting tensions between the cosmological probes, and anomalies in the CMB data, have emerged. These discrepancies have different statistical significance, and although some parts may be due to systematic errors, their persistence strongly indicates possible cracks in the standard ΛCDM cosmological scenario.

Keywords: CMB; dark energy; Hubble tension

Citation: Di Valentino, E. Challenges of the Standard Cosmological Model. *Universe* **2022**, *8*, 399. https://doi.org/10.3390/universe8080399

Academic Editor: Antonino Del Popolo

Received: 30 June 2022
Accepted: 27 July 2022
Published: 29 July 2022

1. Introduction

Among a number of different cosmological models introduced in the literature, the lambda cold dark matter (ΛCDM) scenario is the mathematically simplest model, and has now been practically selected as the "standard" cosmological scenario, because it provides a terrific description of a wide range of astrophysical and cosmological probes in a wide range of scales and epochs. However, despite its fantastic fit to the available observations, ΛCDM contains vast areas of phenomenology and ignorance. For example, it is not yet able to explain key concepts in our understanding of the structure and evolution of the Universe, currently based on three completely unknown quantities that are not expected by theoretical first principles and are not supported by laboratory experiments, although a big effort has been devoted to this research in the recent decades. In actuality, the physical evidence for these unknown pillars comes only from cosmological and astrophysical observations, and the ΛCDM model assumes the simplest assumptions for all of them. We can list these three quantities and their specific solutions for the standard model as follows. First, the inflation [1–3], introduced to solve crucial puzzles of the early evolution of the Universe, in the standard model is given by a single, minimally coupled, slow-rolling scalar field. Second, the dark matter (DM) [4,5] is expected to interact only gravitationally to facilitate the formation of the structures, and in the standard model it is assumed to be pressureless and cold, but there is no direct evidence of DM particles. Third, the dark energy (DE) [6,7] component, introduced to explain the current stage of accelerated expansion, in the standard model is the cosmological constant term Λ, without any strong physical basis.

The standard ΛCDM cosmological model, while hugely successful in explaining the observations, is therefore mainly favoured by its simplicity. Actually, with just six free parameters, it manages to fit well all the current cosmological observations [8–17]. This is a spectacular success, but it must not be forgotten that the model has many weaknesses. For example, it remains a theoretical challenge to understand the magnitude of the cosmological constant Λ from first principles. Deviations from a power law in the primordial spectrum of perturbations are expected in practically all the inflationary scenarios, but are set to zero in the ΛCDM model. The DM can be made of different particles, it could interact, and it can happen to have a non-negligible momentum in certain epochs. The ΛCDM scenario is, therefore, in some ways similar to a phenomenological effective theory, i.e., an approximation to the underlying real model theoretically motivated which has yet to be discovered, and with the improvement in the number and accuracy of the observations,

the deviations from ΛCDM are not unexpected. Thus, discrepancies between key cosmological parameters of the models that have emerged with different statistical significance in recent years could reveal a more complete description of our Universe, bringing new understanding to several areas of physics. Although some of these discrepancies may have a systematic origin, their persistence across probes should require multiple and unrelated errors, strongly suggesting the need for new physics beyond the canonical ΛCDM model.

Current cosmological tensions and anomalies are the subject of the Cosmology Intertwined review paper I submitted for the SNOWMASS [1] call [18], which includes contributions from over 200 people who have participated in brainstorming sessions and provided feedback through regular Zoom seminars and meetings. This White Paper is based on the four letters of interest Ipresented in August 2020 [19–22], which deal with the H_0 disagreement between the cosmic microwave background (CMB) and the local distance ladder measurements [22], the growth tension quantified by the parameter S_8 with the cosmic shear and cluster counts data [19], and a non-zero curvature of the Universe Ω_k [20] related to the $A_{\rm lens}$ problem, which is an internal anomaly of the Planck data. However, one can also find a section where there is room for discussion of many less-well-known less-standard existing signals in cosmological and astrophysical data that seem to be in tension (2σ or more) with the standard ΛCDM model as defined by the Planck 2018 parameter values [12]. In many cases, the signals are controversial and a debate is currently underway in the literature on the possible systematic origin of some of these signals. The reader is invited to take a look at the paper [18] if interested in knowing more.

In this brief short overview paper, I will mainly focus instead on the Hubble constant discussion, and I will conclude with some hints at other curious tensions and anomalies of the current CMB data.

2. The H_0 Tension

The Hubble constant H_0 describes the expansion rate of the Universe today. This can be achieved mainly in two ways: (i) by measuring the luminosity distance and the recessional velocity (or redshift) due to the cosmic expansion of known standard candles, and by computing the proportionality factor (Hubble–Lemaître law), this approach is model-independent and it is based on geometrical measurements; (ii) by considering early Universe probes and, assuming a model for the expansion history of the Universe, estimating the expansion rate today. For example, we have CMB measurements and assume the standard model of cosmology, i.e., the ΛCDM scenario, where the expansion history of the Universe is obtained with the Friedmann's equations.

The H_0 tension is the name given to the 5σ disagreement between the CMB Planck 2018 estimate of the Hubble constant obtained by assuming a standard ΛCDM cosmological model, i.e., $H_0 = 67.27 \pm 0.60$ km/s/Mpc at 68% CL [12], and the local value measured by the SH0ES (Supernova, H_0, for the Equation of State of Dark Energy) collaboration [23], i.e., $H_0 = 73.04 \pm 1.04$ km/s/Mpc at 68% CL, calibrating the Type Ia Supernovae (SNeIa) with the Cepheids.

The latest local measurement obtained by the SH0ES collaboration is based on the distance ladder approach shown in Figure 12 of Ref. [23]. In this plot, one can see that H_0 is measured with a simultaneous fit, performed by optimizing a χ^2 statistic to determine the most probable values of the parameters of a three-rung distance ladder: (i) geometric distance measurements of the anchors used to standardize Cepheid variables (lower left panel), (ii) standardized Cepheids used to calibrate SNeIa in nearby galaxies (middle panel), and (iii) calibrated SNeIa used to obtain the Hubble flow (top right panel).

On the other side, we have, instead, a CMB measurement, i.e., the black body radiation emitted at recombination characterized by extremely small anisotropies (of the order of 10^{-5}). We can expand in Legendre polynomials the two-point correlation function between the difference of temperature in two directions in the sky, averaged over the total sky, and thus obtain the temperature angular power spectrum. At the same time, we can choose a set of parameters describing our theoretical model to compute our theoretical angular

power spectrum, usually with the publicly available Boltzmann solver codes `CAMB` [24] or `CLASS` [25]. Due to the correlations present between the parameters, the variation of different quantities can produce similar effects on the CMB. We can finally compare the angular power spectrum obtained from the data with the one computed by varying the parameters of the model and, using a Bayesian analysis, we obtain the best combination of cosmological parameter values that fits the data. Among the various statistics that can be used to achieve this, the simplest form of the Markov chain Monte Carlo method is widely used, and some of the codes most commonly used by the scientific community are `CosmoMC` [26], `MontePyhton` [27], and `CosmoSIS` [28]. In this way, we can obtain the constraints of the parameters. We can extract four independent angular spectra from a CMB experiment: the autocorrelation of the temperature, type E polarization (density fluctuations), and type B polarization (gravitational waves), and the cross-correlation between the temperature and the type E polarization. If we compare the constraints on the parameters obtained separately for a ΛCDM scenario from Planck EE, TE, and TT high-ℓ power spectra combined with low-ℓ polarization and temperature data, we see a perfect agreement [12], which shows internal consistency between the different independent probes. We can therefore conclude that the 2018 Planck results are a wonderful confirmation of the flat standard ΛCDM cosmological model. However, these results have two important caveats: (1) the cosmological constraints are obtained by assuming a cosmological model, and if we change the assumptions, completely different results can be obtained; (2) these results are affected by the degeneracy between the parameters that induce similar effects on the observables, so that they can be biased towards a correlation direction.

2.1. The H_0 Measurements

Supporting a lower value for the Hubble constant H_0 are the other CMB experiments that assume a ΛCDM cosmological model, such as the ground-based CMB telescope South Pole Telescope (SPT-3G) [29], that finds $H_0 = 68.8 \pm 1.5$ km/s/Mpc at 68% CL, or the Atacama Cosmology Telescope (ACT-DR4) + Wilkinson Microwave Anisotropy Probe (WMAP) [13], which gives $H_0 = 67.6 \pm 1.1$ km/s/Mpc at 68% CL. However, a similar value is also obtained from the baryon acoustic oscillations (BAO) measurements from the BOSS and eBOSS estimates [15] plus the Big Bang nucleosynthesis (BBN) data, which assume a ΛCDM scenario and are CMB-independent. In general, we find that all of the early Universe measurements, assuming a vanilla ΛCDM cosmological scenario for the expansion history, are completely in agreement with a lower value for the Hubble constant today such as that estimated by Planck. An extensive list of all the Hubble constant measurements in the early and late Universe made by different astronomical missions and groups over the years are summarized in Figure 2 of Ref. [18], where the orange vertical band corresponds to the H_0 value measured by the SH0ES team and the light pink vertical band corresponds to the H_0 value as reported by the Planck 2018 team within a ΛCDM scenario [2]. This figure is really busy, with many measurements with error bars so large that do not help discriminate the true value for the Hubble constant, so we filtered it to obtain Figure 1, where we only keep the high-precision measurements of H_0, corresponding to the early Universe estimates with error bars less than 1.5 km/s/Mpc, and the measurements in the late Universe with error bars less than 3.0 km/s/Mpc. In this way we can fully appreciate the high accuracy and consistency of the data at both sides of this plot, and the need for an exact solution (new physics or unrelated errors) that can explain all these multiple observations.

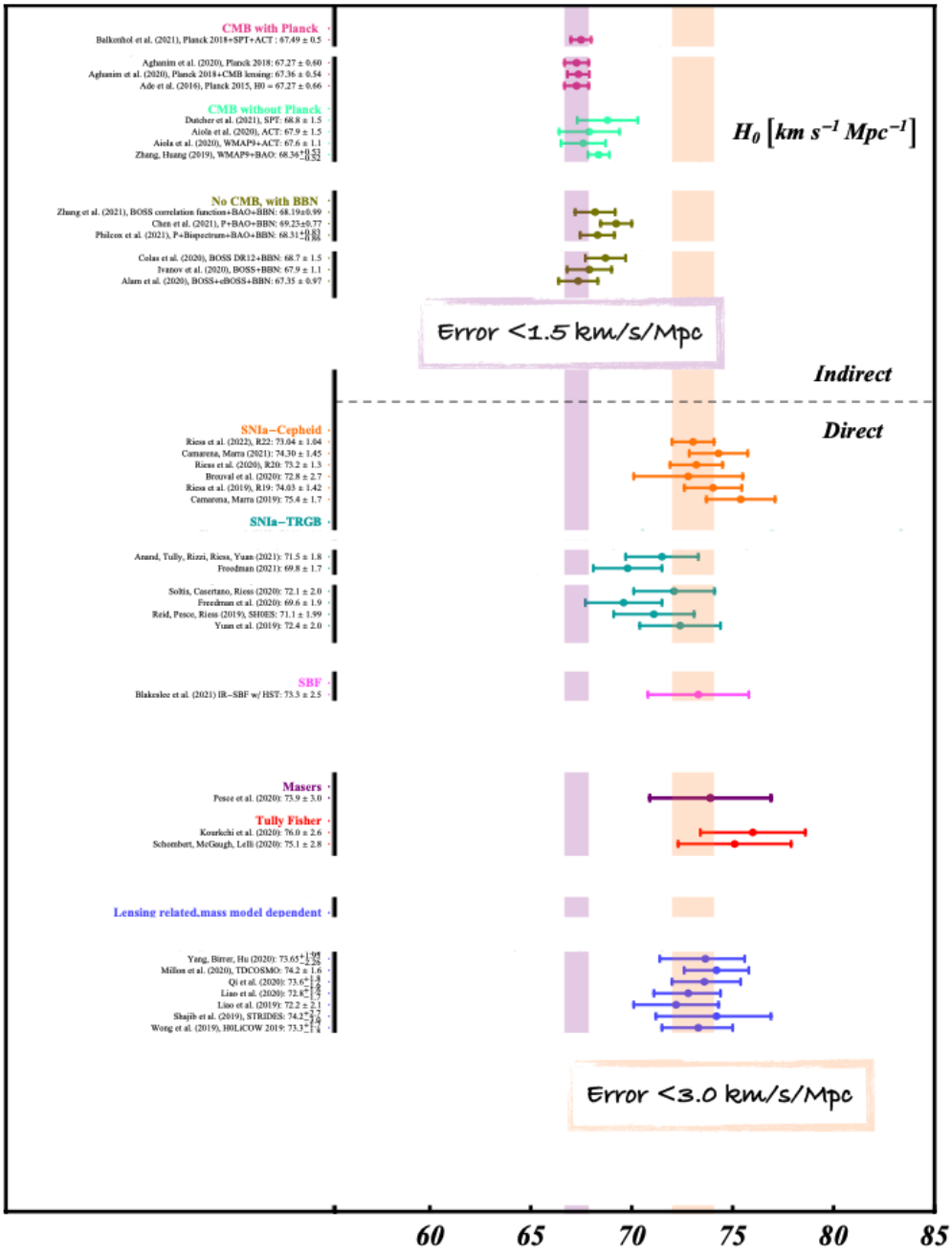

Figure 1. Filtered version of Figure 2 of Ref. [18] with only the high-precision measurements of H_0. For the original figure, details, and references, see Ref. [18].

If we now focus on the late Universe measurements since 2020 of Figure 2 of Ref. [18], we see that they are instead preferring higher values of H_0. We have, in orange, the SNeIa calibrated with Cepheids [23,30–32], as performed by the SH0ES collaboration. Then, we find, in dark green, the SNeIa calibrated with the tip of the red-giant branch (TRGB) [33–38] where, focusing on high-precision measurements, there is the well-discussed Freedman 2021 [33] measurement which is exactly in between the Planck and SH0ES values of H_0, i.e., in agreement with both sides within 1.5σ, and the new independent reanalysis of the targets presented by the Carnegie-Chicago Hubble Program (CCHP) performed in [36] that is shifted more in agreement with the SH0ES value. Then, we see in fuchsia the surface brightness fluctuation (SBF) measurements [39,40], where Ref. [40] uses the SBF to calibrate the SNeIa, while Ref.[39] uses the SBF as a replacement distance ladder for long-range indicator, calibrated by both Cepheids and TRGB that separately give the same

result. Then, we have, in brown, the Type II Supernovae [41,42] used as standardisable candles and calibrated by both Cepheids and TRGB, in purple, the Megamaser Cosmology Project [43], which measures H_0 avoiding any distance ladder and providing the geometric distance directly in the Hubble flow, and in red, the measurements based on the Tully–Fisher relation [44,45] calibrated with both Cepheids and TRGB. Finally, we find, in blue, the strong lensing measurements of the time delays of multiple images of quasar systems caused by the strong gravitational lensing from a foreground galaxy [46–50]. While those based on the H0LiCOW data were more in agreement with SH0ES, the latest TDCOSMO results relax the assumptions on the lens mass density profile, obtaining much weaker bounds, and once combined with SLACS, they shift H_0 towards a lower value. These types of measurements have relaxed bounds on the Hubble constant, which is in agreement with both SH0ES and Planck within 1.5σ, and are highly dependent on the astrophysical model.

In the absence of a full covariance matrix between the late Universe measurements of the Hubble constant discussed before, we can quantify the robustness of the disagreement between the measurements in the early and late Universe using the same conservative approach adopted in Ref. [51], i.e., by computing an arithmetic average of all the late Universe measurements in a colour group, and associating with this average the smaller error bar in the group. After that, we can compute a weighted average of all the results of the different colour groups. If we combine all the values in the references above using this method, we have an optimistic value, which is $H_0 = 72.97 \pm 0.63$ km/s/Mpc at 68% CL, i.e., at about 6.55σ tension with Planck. If we now exclude one colour group of data and take the average with the largest error bars, which is obtained when we exclude the most precise Hubble constant measurement we have, which is based on SNeIa calibrated with Cepheids, we find a conservative estimate that is equal to $H_0 = 72.73 \pm 0.80$ km/s/Mpc at 68% CL, i.e., at about 5.5σ tension with Planck. Finally, if we repeat the process ruling out two colour groups of measurements and choosing the average with the largest error bar, we obtain $H_0 = 73.3 \pm 1.1$ km/s/Mpc at 68% CL in 4.8σ tension with Planck. We call this an ultraconservative estimate obtained by excluding measurements based on SNeIa calibrated with Cepheids and the time-delay lensing data. Therefore, we can conclude that the disagreement is robust and statistically significant, even by removing one or two groups of measurements, and ranges between $\sim$4–6σ (see also [52,53]). In this regard, it was extensively discussed Figure A1 in Ref. [33], where a convergence of the Hubble constant measurements in the last $\sim$40 years is shown. However, what is missing in that plot is an indication of what kind of measurement was obtained with which experiment, because in the past the tension was within the same types of measurements and at the same redshifts and thus indicating directly the presence of systematic errors, while now the puzzling aspect is that there are no late Universe measurements below the early Universe estimates and vice versa. Given the robustness of the tension removing some groups of data and the distribution of the values, it is difficult to find a single type of systematic error that can resolve the Hubble constant tension, and at the same time, it is less probable to have multiple, unrelated systematic errors that bias the Hubble constant values in the same direction, instead of scattering them around the true value.

2.2. Looking for a Solution Beyond Systematic Errors

On the other hand, since the early Universe constraints are model-dependent, we can try to modify the phenomenological ΛCDM standard cosmological model used to analyse the data and see if a new model can work to solve the Hubble constant tension. Many alternative models have been proposed as a solution to the H_0 tension, and many of them are listed in the following review papers: Refs. [18,22,52,54–59]. Usually, the solutions are classified in early solutions, corresponding to modifications of the standard cosmological model before recombination, such as the variation of the effective number of relativistic degrees of freedom $N_{\rm eff}$ [60] or the introduction of an early dark energy (EDE) [61], or late time solutions, corresponding to modifications of the standard cosmological model after recombination, such as exotic dark energy models with an equation of state free to vary [62]

or interacting dark energy scenarios [63]. I will comment on the actual validity of the early vs. late time solutions to solve the Hubble tension in the next subsections, but it can be anticipated that there is currently no consensus on the validity of the models proposed as a solution for the Hubble constant problem.

2.2.1. The $H_0 - r_d$ Plane

If we assume a different model for the expansion history of the Universe and use this model to fit the Planck power spectra, then we can classify the formally successful models in solving the H_0 tension only by comparing the estimated H_0 parameter in the new model with the SH0ES result, as was performed in Table B1 of Ref. [58]. In this case, a model comparison is not performed and the goodness of the fit is not taken into account, but the tension between the H_0 value estimated by Planck assuming a non-standard cosmological scenario ($H_{0,new} \pm \sigma_{H_{0,new}}$) and SH0ES ($H_{0,SH0ES} \pm \sigma_{H_{0,SH0ES}}$) is computed using the formula $T = (H_{0,SH0ES} - H_{0,new})/\sqrt{(\sigma_{H_{0,SH0ES}})^2 + (\sigma_{H_{0,new}})^2}$. We see that most of the successful models with tension T less than 1σ are late time solutions. However, for these models, the inclusion of BAO and Pantheon SNeIa measurements significantly worsens the fit of the data because these scenarios fail to recover the shape of $H(z)$ at low redshifts. In actuality, a combination of BAO and Pantheon data constrains the product of H_0 and the sound horizon r_s, as one can see in Figure 1 of Ref. [54]. This implies that, to have a higher H_0 value from BAO + Pantheon in agreement with SH0ES, we need $r_s \sim 137$ Mpc, while to agree with Planck, assuming ΛCDM, we need $r_s \sim 147$ Mpc. For this reason, the solutions that can increase H_0 and at the same time decrease r_s are most promising. In Figure 3 of Ref. [64], one can see that late time solutions, such as wCDM, increase H_0 because they reduce the expansion history at intermediate redshift, but do not affect the sound horizon r_s. However, early time solutions, such as $N_{\rm eff}$ or EDE, move in the right direction of correlation for both parameters, but cannot fully solve the Hubble constant tension between Planck and SH0ES without including a prior on H_0. In this case, in fact, the best fit obtained by these models is always the ΛCDM one and the reduction of the tension is mainly due to a volume effect due to the increase of the error bars of the parameters. If we now assume a different model for the expansion history of the Universe and use this model to fit a combination of different data, not just Planck, we can now classify the model that formally succeeded in solving the H_0 tension, as was performed in Table B2 of Ref. [58], without considering a model comparison but only computing the tension T. In this case, many of the successful models are early time solutions.

At this point it is worth noting that we should be careful to rule out all the late time solutions due to their disagreement with the BAO data. In actuality, BAO is formed in the early Universe, when baryons are strongly coupled to photons, and the gravitational collapse due to the cold dark matter is counterbalanced by the radiation pressure, but these fluctuations have evolved and we can observe BAO at low redshifts in the distribution of galaxies. Since the data reduction process leading to these measurements requires assumptions about the fiducial cosmology, BAO is model-dependent (see Ref. [65] for a discussion about the BAO dependence on ΛCDM assumptions). In other words, the tension between Planck + BAO, assuming an exotic dark energy model, and SH0ES could be due to a statistical fluctuation in this case. The BAO reliability in extended models was evaluated for early time modifications of the expansion history and DE late time modifications that can be parametrized by $w_0 w_a$ (see Refs. [15,66,67]). Indeed, the whole procedure leading to the BAO dataset performed by the different collaborations may not necessarily be valid in extended DE models, where perturbations in the mildly nonlinear regime are important. For this reason, the BAO data may need to be non-trivially revised on a case-by-case basis when applied to constrain exotic DE cosmologies [3].

2.2.2. The M_B Tension

Furthermore, it was pointed out in Ref. [73] that we should be careful in quantifying the goodness of a model in solving the Hubble tension just by looking at the H_0 estimate

that such a model can provide. In actuality, SH0ES measures the SNeIa absolute magnitude M_B, and to obtain the H_0 value it uses the Hubble flow of the SNeIa in the redshift range $0.023 \leq z \leq 0.15$ and a cosmography with $q_0 = -0.55$ and $j_0 = 1$, which is information beyond the local Universe. This implies that a model with a fast transition at very low redshift ($z < 0.1$), such as a hockey-stick dark energy scenario, can completely solve the Hubble tension, but may disagree with the measured M_B at more than 5σ (see Ref. [32]). Therefore, instead of explaining the H_0 tension, we should deal with the M_B tension. The advantage of using an M_B prior is that the all the information about the shape of the SNeIa magnitude–redshift relation is not lost, and that it is possible to combine, at the same time, the entire SNeIa sample Pantheon without the risk of double-counting the SNeIa used in the Hubble flow. We can now classify successful models in solving the M_B tension, and this was carried out in Table 1 of Ref. [74], where the best solution appears to be a closed Universe with a varying electron mass [75]. Finally, it has been argued that the M_B tension is another reason to rule out modifications of the expansion history at late times: while they can provide a higher H_0 value, these could be strongly disfavoured by the Pantheon magnitude–redshift relation (see Ref. [76]). However, this is true for all the transitions at very low redshift ($z < 0.1$), such as a hockey-stick dark energy scenario, but should be tested on a case-by-case basis for smooth scenarios, where using a H_0 prior or an M_B prior gives the same results, i.e., for those models where the Hubble–Lemaître law is still valid.

2.2.3. The $H_0 - r_d - \Omega_m$ Plane

Finally, we have a further complication: the early time solutions proposed to alleviate the H_0 tension increase the S_8 tension (see the next section). In actuality, a model that simply changes the value of the sound horizon r_d would not completely resolve the tension, as it will affect the inferred value of the matter density Ω_m and transfer the tension to it. Figure 1 of Ref. [56] shows that achieving full agreement between CMB, BAO, and SH0ES through a reduction of r_d requires a higher value of $\Omega_m h^2$ as measured by the CMB, significantly exacerbating the tension with the weak lensing experiments, as shown in Figure 2 of Ref. [56]. Therefore, the tension between the different probes should be considered not only in the plane $H_0 - r_d$, but it should be extended to the triplet of parameters $H_0 - r_d - \Omega_m$. A plot showing the density of the cosmological models proposed to alleviate the Hubble tension can be found in Figure B1 of Ref. [58]. A model in agreement with all available datasets should have a data point that crosses the H_0 value measured by SH0ES (light blue band), the matter density $\Omega_m h^2$ measured by the CMB (light yellow band), and the sound horizon $r_d h$ measured by BAO (light green band), and at the moment, we can safely conclude that there are no specific proposals that prove to be highly probable or far better than all the others.

3. Additional Anomalies and Tensions

3.1. The S_8 Tension

A tension on the S_8 parameter, defined as a combination of the matter density Ω_m and the clustering amplitude of the matter power spectrum σ_8, i.e., $S_8 \equiv \sigma_8 \sqrt{(\Omega_m/0.3)}$, is present between the Planck data and the cosmic shear data, assuming the ΛCDM scenario. This tension is becoming statistically significant and is now at the level of 3.1σ with KiDS-100 [77], that gives $S_8 = 0.766^{+0.020}_{-0.014}$, and 2.5σ with DES-Y3 [78], that gives $S_8 = 0.759^{+0.025}_{-0.025}$, while Planck prefers a higher value for $S_8 = 0.834^{+0.016}_{-0.016}$. Preferring a lower S_8 value, we have all of the late Universe measurements, in particular all the data of weak lensing, galaxy cluster, cluster counts, and redshift space distortions. A plot showing the distribution of the S_8 estimates, with a list of all the references, can be found in Figure 4 of Ref. [18]. Again, similar to the H_0 tension, the puzzling aspect is that there are no late Universe measurements above the CMB estimates and vice versa. A summary of the possible candidates proposed to solve the S_8 tension is present in the review papers [18,19]. However, a systematic error in the Planck data could explain the S_8 tension, as clarified in the next subsection.

3.2. The $A_{\rm lens}$ Anomaly

The path of the CMB photons emitted at recombination is weakly deflected by the gravitational lensing effect along the line of sight due to the presence of massive structures. We can define the lensing amplitude $A_{\rm lens}$ [79] as the rescaling of the lensing potential in the CMB power spectra. If we leave this parameter free to vary, its effect on the power spectrum will be the smoothing of the acoustic peaks when increasing $A_{\rm lens}$. An interesting consistency check, therefore, consists of verifying whether the amplitude of the smoothing effect in the CMB power spectra corresponds to the theoretical expectation $A_{\rm lens} = 1$, and if the amplitude of the smoothing is consistent with that measured by the lensing reconstruction, i.e., the four-point correlation function. In other words, if $A_{\rm lens} = 1$, then the theory is correct; otherwise, we have new physics or systematic errors affecting the results.

Although the Planck lensing reconstruction power spectrum is consistent with the expected amplitude for the ΛCDM model that fits the CMB temperature and polarization power spectra, that is, the Planck lensing measurement is compatible with $A_{\rm lens} = 1$ [80], the distribution of $A_{\rm lens}$ inferred from the CMB power spectra indicates a preference for $A_{\rm lens} > 1$ [12]. The joint TTTEEE likelihood, including the polarization data, shifts the preferred value by TT data down towards $A_{\rm lens} = 1$, but the error also is reduced, increasing the significance of $A_{\rm lens} > 1$ to 2.8σ.[4] The preference for a high $A_{\rm lens} \neq 1$ is not just a volume effect in the full parameter space, because the best fit improves by $\Delta\chi^2 \sim 9$ for the temperature power spectrum, when adding a single degree of freedom $A_{\rm lens}$. In other words, $A_{\rm lens} > 1$ is a failed consistency check of Planck 2018 data.

Furthermore, it was shown in Ref. [82], and confirmed in Ref. [12], that the constraints on some cosmological parameters obtained by assuming ΛCDM from two separate fits of the low-ℓ and the high-ℓ multipoles of the Planck temperature power spectrum data are in tension at more than 2σ level, and that fixing the parameter $A_{\rm lens} = 1.2$, similar to its best fit obtained by Planck, could be a way to resolve this internal disagreement of the two multipole regions, directly indicating a systematic error present in the data.

In addition, if we leave this parameter free to vary, there is a strong correlation between the S_8 parameter and $A_{\rm lens}$ [83], so we can lower S_8 to agree with local measurements once we marginalize over $A_{\rm lens}$ (see also Figure 2 of Ref. [84]). This anomaly $A_{\rm lens} > 1$ is very robust, showing a significance at more than 99% CL even when BAO or SNeIa data are included in the analysis.

In a few words, $A_{\rm lens} \neq 1$ is a failed consistency check of the Planck data, a way to resolve an internal tension of the temperature power spectrum, and a way to alleviate the external disagreement of Planck with the S_8 late Universe measurements. It is worth mentioning that the official position of the Planck collaboration is that this $A_{\rm lens}$ anomaly is only a statistical fluctuation [12,85], so it is not a physical problem. However, the fact that Planck data are failing a consistency check poses some problems on the reliability of the results that are lensing-related (such as the curvature of the Universe or the total neutrino mass), suggesting that they could be influenced by an unsolved systematic in the data, and this presents serious limitations to the precision cosmology.

3.3. The Ω_k Tension

Now we want to understand if, assuming general relativity, there is a physical explanation for the $A_{\rm lens}$ anomaly. In fact, a similar effect seems to be captured by another important parameter, which is the curvature of the Universe. Specifically, Planck 2018 found an indication for a closed Universe [12] at approximately 3.4σ, with a 99% probability region of $-0.095 \leq \Omega_k \leq -0.007$.[5] The first question that we want to answer is whether Planck provides an unbiased and reliable estimate of the curvature of the Universe. This may not be the case, as there is a "geometrical degeneracy" with Ω_m that could skew the results. However, since gravitational lensing depends on the matter density, its detection in the CMB power spectra breaks the geometrical degeneracy and, using simulated Planck measurements, it was shown in Ref. [86] that such an experiment could constrain the curvature of the Universe to be flat with an uncertainty of 2%, with no significant

bias towards closed models. Planck therefore prefers a closed Universe ($\Omega_k < 0$) with a probability of 99.985%, and this is not entirely a volume effect, as the best-fit $\Delta\chi^2$ changes by -11 compared to the base ΛCDM when adding one additional degree of freedom as the curvature parameter. The improvement is due also to the fact that the observed low CMB anisotropy quadrupole could be in agreement with a large-scale cut-off in the primordial density fluctuations, as predicted by closed models. Therefore, a model with $\Omega_k < 0$ is slightly preferred over a flat model with $A_{\rm lens} > 1$, because closed models better fit not only the smoothing of the peaks in the damping tail, but also the low-multipole data. A lower quadrupole than that predicted by the ΛCDM scenario was already present in the WMAP data, and a closed Universe to explain this effect was already proposed in Ref. [87].

A joint constraint Planck + lensing + BAO is instead very consistent with a flat Universe, finding $\Omega_k = 0.0007 \pm 0.0019$ at 68% CL [12] ($\Omega_k = 0.0004 \pm 0.0019$ at 68% CL using the alternative likelihood [88]). Given the significant change in the conclusions from Planck alone, it is mandatory to investigate whether the datasets combined together are indeed consistent. In fact, a fundamental prerequisite for combining complementary probes is that they derive from the same cosmological model and therefore must be consistent. While in a ΛCDM model the BAO data agree very well with the Planck measurements (see Figure 1 of Ref. [12]), when we let the curvature vary there is a strong $> 3\sigma$ disagreement between the Planck constraints and the BAO measurements (see Figure 4 of Ref. [86]). The same disagreement is evident in the independent analysis shown in Figure 1 of Ref. [89], as well as in Figure 1 of Ref. [90], which reports a similar tension with the full-shape (FS) galaxy power spectrum measurements from the BOSS DR12 CMASS sample.

The closed models have substantially higher lensing amplitudes than in the ΛCDM model, because a closed Universe means more matter and therefore more lensing. This is why varying Ω_k or $A_{\rm lens}$ gives a similar best fit of the lensing reconstruction data (see Figure 5 of Ref. [86]). There is clearly a degeneracy between the curvature and the $A_{\rm lens}$ parameters, as shown in Figure 2 of Ref. [86], and we can see how fixing the Universe to be flat leads to this anomalous value for $A_{\rm lens} > 1$, while $A_{\rm lens}$ can be in agreement with its expected value if we are open to the possibility of a closed Universe. However, we should be extremely careful in comparing these parameters, because while the $A_{\rm lens}$ parameter is just a phenomenological consistency check that is failing, without any theoretical motivation, the curvature of the Universe is not new physics beyond the standard model [91], but it is predicted by general relativity, and depends on the energy content of the Universe. Furthermore, similarly to what happens with $A_{\rm lens}$, in a closed Universe with $\Omega_k = -0.045$, which is the preferred value for the best fit of the Planck data, the cosmological parameters obtained from the fit of the low-ℓ and the high-ℓ multipoles of the Planck data are now fully compatible. The problem is that by varying Ω_k, both the well-known tensions on H_0 and S_8 are exacerbated: in a ΛCDM + Ω_k model, Planck gives $H_0 = 54.4^{+3.3}_{-4.0}$ km/s/Mpc at 68% CL, increasing the tension with SH0ES at 5.5σ, and S_8 in disagreement at about 3.8σ with KiDS-1000 [77], and more than 3.5σ with DES-Y3 [78].

The compatibility of non-CMB data combinations with a closed Universe was also investigated in Ref. [86], finding that BAO + SNeIa + BBN gives $H_0 = 79.6 \pm 6.8$ km/s/Mpc at 68% CL, perfectly consistent with SH0ES, but at 3.4σ tension with Planck, and that BAO + SNeIa + BBN + SH0ES gives $\Omega_k = -0.091 \pm 0.037$ at 68% CL, i.e., slightly preferring a closed Universe. Furthermore, Ref. [65] uses effective field theories of large-scale structure (EFTofLSS) to constrain Ω_k independently of some flatness assumptions that usually go into different large-scale structure analyses, and finds $\Omega_k = -0.089^{+0.049}_{-0.046}$ at 68% CL, but still agrees with a flat Universe when CMB data are included.

In order to test the robustness of different dataset combinations in preferring a flat Universe, we can extend the parameter space to include variation in the dark energy equation of state. In Ref. [92], it was shown that Planck data are in perfect agreement with the SNeIa and the local Hubble constant measurements, even by strongly preferring a closed Universe, while Planck is still in strong tension with the BAO measurements, so their combination should be considered with some caution. Therefore, the conclusions of a

closed Universe incompatible with the luminosity distance measurements are a result of the assumption of a cosmological constant. In practice, Planck plus the luminosity distance measurements disagree with both a cosmological constant and a flat Universe at more than 99% CL, preferring a phantom closed Universe with the same statistical significance.

This whole debate over the curvature of the Universe has grown to question whether and how the choice of data type affects the parameter constraints, and has stimulated the investigation of how data should be safely chosen and combined in the data analysis to obtain physically meaningful results (see, for example, Ref. [93]).

3.4. The CMB Ground-Based Experiments

On the other hand, if we consider the alternative CMB experiments, we see that ACT-DR4 + WMAP gives at 68% CL $\Omega_k = -0.001 \pm 0.012$ [13] (see also the left panel of Figure 2), while SPT-3G finds $\Omega_k = 0.001^{+0.018}_{-0.019}$ [14]. This is a confirmation that it is possible to obtain precise measurements of Ω_k from a CMB experiment, as suggested by the simulations in Ref. [86], because the gravitational lensing that can be measured by the power spectra depends on the matter density, and its detection breaks the geometrical degeneracy. For these datasets, there is perfect agreement between the CMB and BAO data when the curvature is free to vary, as shown in the right panel of Figure 2, so they can be safely combined together.

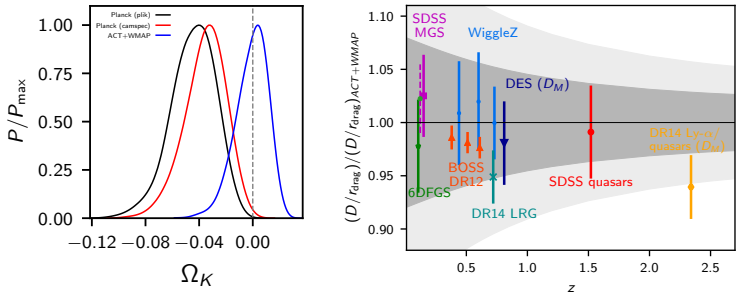

Figure 2. Comparison between Planck and ACT-DR4 (**left panel**) and ACT-DR4 and BAO (**right panel**) assuming a closed Universe.

The significant difference in the estimates of the curvature between Planck and the ground-based CMB telescopes is due to their mutual tension. It is possible to compute the global tensions between these CMB datasets using the suspiciousness statistics [94], finding that between Planck and ACT there is a tension at 2.6σ level, assuming a ΛCDM model. While some parameters can have a larger disagreement over 3σ, this global 2.6σ tension is intriguing because they are looking at the same observable and are assuming the same standard ΛCDM scenario to analyse the data.

If they have such a large difference assuming the standard cosmological model, the tension between Planck and ACT-DR4 can increase even more when considering an extended scenario. In particular, they disagree significantly when a running $\alpha_s = (dn_s/d\log k)$ and a running of the running $\beta_s = (d\alpha_s/d\log k)$ of the scalar spectral index n_s are free to vary: ACT-DR4 + WMAP prefer both these parameters to be different from zero at the level of 2.9σ and 2.7σ, respectively [95], while for Planck they are consistent with zero.

Furthermore, Planck and ACT-DR4 disagree on the results for the early dark energy scenario [96], which is mostly known to be a promising candidate in resolving the Hubble tension: considering ACT-only data or combined with Planck TT up to multipoles 650, there is evidence for EDE $> 3\sigma$, which completely solves the Hubble tension [96,97]. Moreover, the evidence for EDE $> 3\sigma$ persists with the inclusion of Planck lensing and BAO data (shifting H_0 towards a lower value, but still able to alleviate the tension), but it disappears completely once the full Planck multipoles data are considered, with H_0 in tension again with SH0ES. In a few words, the Planck damping tail is at odds with EDE different from zero.

Finally, Planck and ACT-DR4 (and SPT-3G) are in tension for the neutrino sector, both for the neutrino effective number $N_{\rm eff}$ and the total neutrino mass Σm_ν constraints. In particular, in Ref. [98], it was shown that ACT-DR4 + WMAP slightly suggests a neutrino mass with $\Sigma m_\nu = 0.68 \pm 0.31$ eV at 68% CL, and SPT-3G + WMAP prefers $\Sigma m_\nu = 0.46^{+0.14}_{-0.36}$ eV at 68% CL, and both agree with the Planck + CMB lensing constraint of $\Sigma m_\nu = 0.41^{+0.17}_{-0.25}$ eV at 68% CL obtained by marginalizing over $A_{\rm lens}$, which is the possible systematic effect in the Planck data. Furthermore, by extending the parameter space to include variations in the DE and inflationary sector, Ref. [98] finds that both ACT-DR4 and SPT-3G can accommodate larger neutrino masses, and that the anticorrelation present between Σm_ν and H_0 in a ΛCDM framework disappears (see Figure 3 of Ref. [98]). This extended parameter space with a non-zero total neutrino mass is in agreement with the Hubble constant measured locally and can also relieve the S_8 tension.

4. Conclusions

Most of the anomalies and tensions involve the CMB data, and we currently have (i) the 5σ Hubble constant disagreement between the CMB data and the local measurements, (ii) the $2-3\sigma$ S_8 tension between the CMB data and the late Universe measurements, (iii) an anomalous $2-3\sigma$ indication for an excess of lensing $A_{\rm lens}$ in the Planck data, corresponding to a 3σ indication for a closed Universe $\Omega_k < 0$, (iv) a $2-3\sigma$ indication for a running α_s and a running of the running β_s of the scalar spectral index n_s from ACT-DR4 and SPT-3G data, (v) an indication for a total neutrino mass different from zero from ACT-DR4 and SPT-3G, and, finally, (vi) an indication of a $> 3\sigma$ for an EDE for ACT-DR4. These anomalies and tensions present a serious limitation to "precision cosmology" and question whether the CMB results are a confirmation of the flat standard ΛCDM cosmological model. At this point, given the quality of all the analyses, these discrepancies could indicate a problem with the underlying cosmology and our understanding of the Universe, requiring new observations and stimulating the investigation of alternative theoretical models and solutions.

Funding: EDV is supported by a Royal Society Dorothy Hodgkin Research Fellowship.

Institutional Review Board Statement: Not applicable.

Informed Consent Statement: Not applicable.

Data Availability Statement: No new data are used.

Conflicts of Interest: The author declares no conflicts of interest.

Notes

1 The SNOWMASS planning exercise (https://snowmass21.org/start, accessed on 2 July 2022) is a scientific study aimed at identifying the long-term strategy of the particle physics community in the US. This is usually followed by a project prioritization panel to provide specific recommendations for funding agencies.

2 A sample code for producing similar figures with any choice of the data is made publicly available online at github.com/lucavisinelli/H0TensionRealm, accessed on 2 July 2022) .

3 It is worth mentioning here that there are treatments of BAO that make them less model-dependent but with larger error bars, such as the so-called angular two-point BAO correlation function [68–72].

4 It was recently shown in Ref. [81] that the significance of $A_{\rm lens} > 1$ seems to be reduced in the new Planck PR4 release with CamSpec. However, looking at Table 6 of Ref. [81], it is clear that the problem in the temperature power spectrum is not solved and the significance of $A_{\rm lens} > 1$ is unchanged for this probe, but the reduction of its significance is due to the modification of the EE power spectrum, which is shifting all the parameters towards ΛCDM. However, this change in EE is also producing a significant shift in the acoustic scale parameter θ (see Figure 15 of Ref. [81]), and a tension at more than 3σ between TT and EE, but more significantly, the reduced χ^2 values show a more than 4σ tension with the best-fit TT and TTTEEE LCDM model, as shown in Table 1 of Ref. [81].

5 Again, as discussed in the previous footnote, looking at Table 6 of Ref. [81], it is clear that the significance of $\Omega_k < 0$ from the temperature power spectrum is mostly unchanged for the new PR4 release with CamSpec.

References

1. Brout, R.; Englert, F.; Gunzig, E. The Creation of the Universe as a Quantum Phenomenon. *Ann. Phys.* **1978**, *115*, 78. [CrossRef]
2. Guth, A.H. The Inflationary Universe: A Possible Solution to the Horizon and Flatness Problems. *Phys. Rev. D* **1981**, *23*, 347–356. [CrossRef]
3. Sato, K. First Order Phase Transition of a Vacuum and Expansion of the Universe. *Mon. Not. R. Astron. Soc.* **1981**, *195*, 467–479. [CrossRef]
4. Rubin, V.C.; Ford, W.K., Jr. Rotation of the Andromeda Nebula from a Spectroscopic Survey of Emission Regions. *Astrophys. J.* **1970**, *159*, 379–403. [CrossRef]
5. Trimble, V. Existence and Nature of Dark Matter in the Universe. *Ann. Rev. Astron. Astrophys.* **1987**, *25*, 425–472. [CrossRef]
6. Riess, A.G. et al. [Supernova Search Team]. Observational evidence from supernovae for an accelerating universe and a cosmological constant. *Astron. J.* **1998**, *116*, 1009–1038. [CrossRef]
7. Perlmutter, S. et al. [Supernova Cosmology Project]. Measurements of Ω and Λ from 42 high redshift supernovae. *Astrophys. J.* **1999**, *517*, 565–586. [CrossRef]
8. Hinshaw, G. et al. [WMAP]. Nine-Year Wilkinson Microwave Anisotropy Probe (WMAP) Observations: Cosmological Parameter Results. *Astrophys. J. Suppl.* **2013**, *208*, 19. [CrossRef]
9. Beutler, F.; Blake, C.; Colless, M.; Jones, D.H.; Staveley-Smith, L.; Campbell, L.; Parker, Q.; Saunders, W.; Watson, F. The 6dF Galaxy Survey: Baryon Acoustic Oscillations and the Local Hubble Constant. *Mon. Not. R. Astron. Soc.* **2011**, *416*, 3017–3032. [CrossRef]
10. Ross, A.J.; Samushia, L.; Howlett, C.; Percival, W.J.; Burden, A.; Manera, M. The clustering of the SDSS DR7 main Galaxy sample—I. A 4 per cent distance measure at $z = 0.15$. *Mon. Not. R. Astron. Soc.* **2015**, *449*, 835–847. [CrossRef]
11. Alam, S. et al. [BOSS]. The clustering of galaxies in the completed SDSS-III Baryon Oscillation Spectroscopic Survey: Cosmological analysis of the DR12 galaxy sample. *Mon. Not. R. Astron. Soc.* **2017**, *470*, 2617–2652. [CrossRef]
12. Aghanim, N. et al. [Planck]. Planck 2018 results. VI. Cosmological parameters. *Astron. Astrophys.* **2020**, *641*, A6; Erratum: *Astron. Astrophys.* **2021**, *652*, C4. [CrossRef]
13. Aiola, S. et al. [ACT]. The Atacama Cosmology Telescope: DR4 Maps and Cosmological Parameters. *J. Cosmol. Astropart. Phys.* **2020**, 12, 047. [CrossRef]
14. Balkenhol, L. et al. [SPT-3G]. Constraints on ΛCDM extensions from the SPT-3G 2018 EE and TE power spectra. *Phys. Rev. D* **2021**, *104*, 083509. [CrossRef]
15. Alam, S. et al. [eBOSS]. Completed SDSS-IV extended Baryon Oscillation Spectroscopic Survey: Cosmological implications from two decades of spectroscopic surveys at the Apache Point Observatory. *Phys. Rev. D* **2021**, *103*, 083533. [CrossRef]
16. Abbott, T.M.C. et al. [DES]. Dark Energy Survey Year 3 Results: Constraints on extensions to ΛCDM with weak lensing and galaxy clustering. *arXiv* **2022**, arXiv:2207.05766.
17. Abbott, T.M.C. et al. [DES]. Dark Energy Survey Year 3 results: Cosmological constraints from galaxy clustering and weak lensing. *Phys. Rev. D* **2022**, *105*, 023520. [CrossRef]
18. Abdalla, E.; Abellán, G.F.; Aboubrahim, A.; Agnello, A.; Akarsu, O.; Akrami, Y.; Alestas, G.; Aloni, D.; Amendola, L.; Anchordoqui, L.A.; et al. Cosmology intertwined: A review of the particle physics, astrophysics, and cosmology associated with the cosmological tensions and anomalies. *J. High Energy Astrophys.* **2022**, *34*, 49–211. [CrossRef]
19. Di Valentino, E.; Anchordoqui, L.A.; Akarsu, Ö.; Ali-Haimoud, Y.; Amendola, L.; Arendse, N.; Asgari, M.; Ballardini, M.; Basilakos, S.; Battistelli, E.; et al. Cosmology intertwined III: $f\sigma_8$ and S_8. *Astropart. Phys.* **2021**, *131*, 102604. [CrossRef]
20. Di Valentino, E.; Anchordoqui, L.A.; Akarsu, Ö.; Ali-Haimoud, Y.; Amendola, L.; Arendse, N.; Asgari, M.; Ballardini, M.; Basilakos, S.; Battistelli, E.; et al. Snowmass2021—Letter of interest cosmology intertwined IV: The age of the Universe and its curvature. *Astropart. Phys.* **2021**, *131*, 102607. [CrossRef]
21. Di Valentino, E.; Anchordoqui, L.A.; Akarsu, O.; Ali-Haimoud, Y.; Amendola, L.; Arendse, N.; Asgari, M.; Ballardini, M.; Basilakos, S.; Battistelli, E.; et al. Snowmass2021—Letter of interest cosmology intertwined I: Perspectives for the next decade. *Astropart. Phys.* **2021**, *131*, 102606. [CrossRef]
22. Di Valentino, E.; Anchordoqui, L.A.; Akarsu, O.; Ali-Haimoud, Y.; Amendola, L.; Arendse, N.; Asgari, M.; Ballardini, M.; Basilakos, S.; Battistelli, E.; et al. Snowmass2021—Letter of interest cosmology intertwined II: The hubble constant tension. *Astropart. Phys.* **2021**, *131*, 102605. [CrossRef]
23. Riess, A.G.; Yuan, W.; Macri, L.M.; Scolnic, D.; Brout, D.; Casertano, S.; Jones, D.O.; Murakami, Y.; Breuval, L.; Brink, T.G.; et al. A Comprehensive Measurement of the Local Value of the Hubble Constant with 1 km/s/Mpc Uncertainty from the Hubble Space Telescope and the SH0ES Team. *arXiv* **2021**, arXiv:2112.04510.
24. Lewis, A.; Challinor, A.; Lasenby, A. Efficient computation of CMB anisotropies in closed FRW models. *Astrophys. J.* **2000**, *538*, 473–476. [CrossRef]
25. Blas, D.; Lesgourgues, J.; Tram, T. The Cosmic Linear Anisotropy Solving System (CLASS) II: Approximation schemes. *J. Cosmol. Astropart. Phys.* **2011**, *7*, 034. [CrossRef]
26. Lewis, A.; Bridle, S. Cosmological parameters from CMB and other data: A Monte Carlo approach. *Phys. Rev. D* **2002**, *66*, 103511. [CrossRef]
27. Brinckmann, T.; Lesgourgues, J. MontePython 3: Boosted MCMC sampler and other features. *Phys. Dark Univ.* **2019**, *24*, 100260. [CrossRef]

28. Zuntz, J.; Paterno, M.; Jennings, E.; Rudd, D.; Manzotti, A.; Dodelson, S.; Bridle, S.; Sehrish, S.; Kowalkowski, J. CosmoSIS: Modular cosmological parameter estimation. *Astron. Comput.* **2015**, *12*, 45–59. [CrossRef]
29. Dutcher, D. et al. [SPT-3G]. Measurements of the E-mode polarization and temperature-E-mode correlation of the CMB from SPT-3G 2018 data. *Phys. Rev. D* **2021**, *104*, 022003. [CrossRef]
30. Riess, A.G.; Casertano, S.; Yuan, W.; Bowers, J.B.; Macri, L.; Zinn, J.C.; Scolnic, D. Cosmic Distances Calibrated to 1% Precision with Gaia EDR3 Parallaxes and Hubble Space Telescope Photometry of 75 Milky Way Cepheids Confirm Tension with ΛCDM. *Astrophys. J. Lett.* **2021**, *908*, L6. [CrossRef]
31. Breuval, L.; Kervella, P.; Anderson, R.I.; Riess, A.G.; Arenou, F.; Trahin, B.; Mérand, A.; Gallenne, A.; Gieren, W.; Storm, J.; et al. The Milky Way Cepheid Leavitt law based on Gaia DR2 parallaxes of companion stars and host open cluster populations. *Astron. Astrophys.* **2020**, *643*, A115. [CrossRef]
32. Camarena, D.; Marra, V. On the use of the local prior on the absolute magnitude of Type Ia supernovae in cosmological inference. *Mon. Not. R. Astron. Soc.* **2021**, *504*, 5164–5171. [CrossRef]
33. Freedman, W.L. Measurements of the Hubble Constant: Tensions in Perspective. *Astrophys. J.* **2021**, *919*, 16. [CrossRef]
34. Soltis, J.; Casertano, S.; Riess, A.G. The Parallax of ω Centauri Measured from Gaia EDR3 and a Direct, Geometric Calibration of the Tip of the Red Giant Branch and the Hubble Constant. *Astrophys. J. Lett.* **2021**, *908*, L5. [CrossRef]
35. Freedman, W.L.; Madore, B.F.; Hoyt, T.; Jang, I.S.; Beaton, R.; Lee, M.G.; Monson, A.; Neeley, J.; Rich, J. Calibration of the Tip of the Red Giant Branch (TRGB). *arXiv* **2020**, arXiv:2002.01550.
36. Anand, G.S.; Tully, R.B.; Rizzi, L.; Riess, A.G.; Yuan, W. Comparing Tip of the Red Giant Branch Distance Scales: An Independent Reduction of the Carnegie-Chicago Hubble Program and the Value of the Hubble Constant. *Astrophys. J.* **2022**, *932*, 15. [CrossRef]
37. Jones, D.O.; Mandel, K.S.; Kirshner, R.P.; Thorp, S.; Challis, P.M.; Avelino, A.; Brout, D.; Burns, C.; Foley, R.J.; Pan, Y.C.; et al. Cosmological Results from the RAISIN Survey: Using Type Ia Supernovae in the Near Infrared as a Novel Path to Measure the Dark Energy Equation of State. *arXiv* **2022**, arXiv:2201.07801.
38. Dhawan, S.; Goobar, A.; Johansson, J.; Jang, I.S.; Rigault, M.; Harvey, L.; Maguire, K.; Freedman, W.L.; Madore, B.F.; Smith, M.; et al. A Uniform Type Ia Supernova Distance Ladder with the Zwicky Transient Facility: Absolute Calibration Based on the Tip of the Red Giant Branch (TRGB) Method. *arXiv* **2022**, arXiv:2203.04241.
39. Blakeslee, J.P.; Jensen, J.B.; Ma, C.P.; Milne, P.A.; Greene, J.E. The Hubble Constant from Infrared Surface Brightness Fluctuation Distances. *Astrophys. J.* **2021**, *911*, 65. [CrossRef]
40. Khetan, N.; Izzo, L.; Branchesi, M.; Wojtak, R.; Cantiello, M.; Murugeshan, C.; Agnello, A.; Valle, M.D.; Gall, C.; Hjorth, J.; et al. A new measurement of the Hubble constant using Type Ia supernovae calibrated with surface brightness fluctuations. *Astron. Astrophys.* **2021**, *647*, A72. [CrossRef]
41. de Jaeger, T.; Stahl, B.E.; Zheng, W.; Filippenko, A.V.; Riess, A.G.; Galbany, L. A measurement of the Hubble constant from Type II supernovae. *Mon. Not. R. Astron. Soc.* **2020**, *496*, 3402–3411. [CrossRef]
42. de Jaeger, T.; Galbany, L.; Riess, A.G.; Stahl, B.E.; Shappee, B.J.; Filippenko, A.V.; Zheng, W. A 5% measurement of the Hubble constant from Type II supernovae. *arXiv* **2022**, arXiv:2203.08974.
43. Pesce, D.W.; Braatz, J.A.; Reid, M.J.; Riess, A.G.; Scolnic, D.; Condon, J.J.; Gao, F.; Henkel, C.; Impellizzeri, C.M.V.; Kuo, C.Y.; et al. The Megamaser Cosmology Project. XIII. Combined Hubble constant constraints. *Astrophys. J. Lett.* **2020**, *891*, L1. [CrossRef]
44. Kourkchi, E.; Tully, R.B.; Anand, G.S.; Courtois, H.M.; Dupuy, A.; Neill, J.D.; Rizzi, L.; Seibert, M. Cosmicflows-4: The Calibration of Optical and Infrared Tully–Fisher Relations. *Astrophys. J.* **2020**, *896*, 3. [CrossRef]
45. Schombert, J.; McGaugh, S.; Lelli, F. Using the Baryonic Tully–Fisher Relation to Measure Ho. *Astron. J.* **2020**, *160*, 71. [CrossRef]
46. Liao, K.; Shafieloo, A.; Keeley, R.E.; Linder, E.V. Determining Model-independent H_0 and Consistency Tests. *Astrophys. J. Lett.* **2020**, *895*, L29. [CrossRef]
47. Qi, J.Z.; Zhao, J.W.; Cao, S.; Biesiada, M.; Liu, Y. Measurements of the Hubble constant and cosmic curvature with quasars: Ultracompact radio structure and strong gravitational lensing. *Mon. Not. R. Astron. Soc.* **2021**, *503*, 2179–2186. [CrossRef]
48. Yang, T.; Birrer, S.; Hu, B. The first simultaneous measurement of Hubble constant and post-Newtonian parameter from Time-Delay Strong Lensing. *Mon. Not. R. Astron. Soc.* **2020**, *497*, L56–L61. [CrossRef]
49. Birrer, S.; Shajib, A.J.; Galan, A.; Millon, M.; Treu, T.; Agnello, A.; Auger, M.; Chen, G.C.F.; Christensen, L.; Collett, T.; et al. TDCOSMO—IV. Hierarchical time-delay cosmography—Joint inference of the Hubble constant and galaxy density profiles. *Astron. Astrophys.* **2020**, *643*, A165. [CrossRef]
50. Denzel, P.; Coles, J.P.; Saha, P.; Williams, L.L.R. The Hubble constant from eight time-delay galaxy lenses. *Mon. Not. R. Astron. Soc.* **2021**, *501*, 784–801. [CrossRef]
51. Di Valentino, E. A combined analysis of the H_0 late time direct measurements and the impact on the Dark Energy sector. *Mon. Not. R. Astron. Soc.* **2021**, *502*, 2065–2073. [CrossRef]
52. Verde, L.; Treu, T.; Riess, A.G. Tensions between the Early and the Late Universe. *Nat. Astron.* **2019**, *3*, 891. [CrossRef]
53. Riess, A.G. The Expansion of the Universe is Faster than Expected. *Nat. Rev. Phys.* **2019**, *2*, 10–12. [CrossRef]
54. Knox, L.; Millea, M. Hubble constant hunter's guide. *Phys. Rev. D* **2020**, *101*, 043533. [CrossRef]
55. Di Valentino, E. The H_0 Tensions to Discriminate Among Concurring Models. In *Modified Gravity and Cosmology*; Springer: Cham, Switzerland, 2021. [CrossRef]
56. Jedamzik, K.; Pogosian, L.; Zhao, G.B. Why reducing the cosmic sound horizon alone can not fully resolve the Hubble tension. *Commun. Phys.* **2021**, *4*, 123. [CrossRef]

57. Perivolaropoulos, L.; Skara, F. Challenges for ΛCDM: An update. *arXiv* **2021**, arXiv:2105.05208.
58. Di Valentino, E.; Mena, O.; Pan, S.; Visinelli, L.; Yang, W.; Melchiorri, A.; Mota, D.F.; Riess, A.G.; Silk, J. In the realm of the Hubble tension—A review of solutions. *Class. Quant. Grav.* **2021**, *38*, 153001. [CrossRef]
59. Shah, P.; Lemos, P.; Lahav, O. A buyer's guide to the Hubble constant. *Astron. Astrophys. Rev.* **2021**, *29*, 9. [CrossRef]
60. Vagnozzi, S. New physics in light of the H_0 tension: An alternative view. *Phys. Rev. D* **2020**, *102*, 023518. [CrossRef]
61. Poulin, V.; Smith, T.L.; Karwal, T.; Kamionkowski, M. Early Dark Energy Can Resolve The Hubble Tension. *Phys. Rev. Lett.* **2019**, *122*, 221301. [CrossRef]
62. Di Valentino, E.; Melchiorri, A.; Silk, J. Reconciling Planck with the local value of H_0 in extended parameter space. *Phys. Lett. B* **2016**, *761*, 242–246. [CrossRef]
63. Di Valentino, E.; Melchiorri, A.; Mena, O.; Vagnozzi, S. Interacting dark energy in the early 2020s: A promising solution to the H_0 and cosmic shear tensions. *Phys. Dark Univ.* **2020**, *30*, 100666. [CrossRef]
64. Arendse, N.; Wojtak, R.J.; Agnello, A.; Chen, G.C.F.; Fassnacht, C.D.; Sluse, D.; Hilbert, S.; Millon, M.; Bonvin, V.; Wong, K.C.; et al. Cosmic dissonance: Are new physics or systematics behind a short sound horizon? *Astron. Astrophys.* **2020**, *639*, A57. [CrossRef]
65. Glanville, A.; Howlett, C.; Davis, T.M. Full-Shape Galaxy Power Spectra and the Curvature Tension. *arXiv* **2022**, arXiv:2205.05892.
66. Heinesen, A.; Blake, C.; Wiltshire, D.L. Quantifying the accuracy of the Alcock-Paczyński scaling of baryon acoustic oscillation measurements. *J. Cosmol. Astropart. Phys.* **2020**, *1*, 038. [CrossRef]
67. Bernal, J.L.; Smith, T.L.; Boddy, K.K.; Kamionkowski, M. Robustness of baryon acoustic oscillation constraints for early-Universe modifications of ΛCDM cosmology. *Phys. Rev. D* **2020**, *102*, 123515. [CrossRef]
68. Sanchez, E.; Carnero, A.; Garcia-Bellido, J.; Gaztanaga, E.; de Simoni, F.; Crocce, M.; Cabre, A.; Fosalba, P.; Alonso, D. Tracing The Sound Horizon Scale With Photometric Redshift Surveys. *Mon. Not. R. Astron. Soc.* **2011**, *411*, 277–288. [CrossRef]
69. Carvalho, G.C.; Bernui, A.; Benetti, M.; Carvalho, J.C.; Alcaniz, J.S. Baryon Acoustic Oscillations from the SDSS DR10 galaxies angular correlation function. *Phys. Rev. D* **2016**, *93*, 023530. [CrossRef]
70. Alcaniz, J.S.; Carvalho, G.C.; Bernui, A.; Carvalho, J.C.; Benetti, M. Measuring baryon acoustic oscillations with angular two-point correlation function. *Fundam. Theor. Phys.* **2017**, *187*, 11–19. [CrossRef]
71. de Carvalho, E.; Bernui, A.; Carvalho, G.C.; Novaes, C.P.; Xavier, H.S. Angular Baryon Acoustic Oscillation measure at $z = 2.225$ from the SDSS quasar survey. *J. Cosmol. Astropart. Phys.* **2018**, *4*, 064. [CrossRef]
72. Carvalho, G.C.; Bernui, A.; Benetti, M.; Carvalho, J.C.; de Carvalho, E.; Alcaniz, J.S. The transverse baryonic acoustic scale from the SDSS DR11 galaxies. *Astropart. Phys.* **2020**, *119*, 102432. [CrossRef]
73. Camarena, D.; Marra, V. Local determination of the Hubble constant and the deceleration parameter. *Phys. Rev. Res.* **2020**, *2*, 013028. [CrossRef]
74. Schöneberg, N.; Abellán, G.F.; Sánchez, A.P.; Witte, S.J.; Poulin, V.; Lesgourgues, J. The H_0 Olympics: A fair ranking of proposed models. *arXiv* **2021**, arXiv:2107.10291.
75. Sekiguchi, T.; Takahashi, T. Early recombination as a solution to the H_0 tension. *Phys. Rev. D* **2021**, *103*, 083507. [CrossRef]
76. Efstathiou, G. To H_0 or not to H_0? *Mon. Not. R. Astron. Soc.* **2021**, *505*, 3866–3872. [CrossRef]
77. Heymans, C.; Tröster, T.; Asgari, M.; Blake, C.; Hildebrandt, H.; Joachimi, B.; Kuijken, K.; Lin, C.A.; Sánchez, A.G.; van den Busch, J.L.; et al. KiDS-1000 Cosmology: Multi-probe weak gravitational lensing and spectroscopic galaxy clustering constraints. *Astron. Astrophys.* **2021**, *646*, A140. [CrossRef]
78. Amon, A. et al. [DES]. Dark Energy Survey Year 3 results: Cosmology from cosmic shear and robustness to data calibration. *Phys. Rev. D* **2022**, *105*, 023514. [CrossRef]
79. Calabrese, E.; Slosar, A.; Melchiorri, A.; Smoot, G.F.; Zahn, O. Cosmic Microwave Weak lensing data as a test for the dark universe. *Phys. Rev. D* **2008**, *77*, 123531. [CrossRef]
80. Aghanim, N. et al. [Planck]. Planck 2018 results. VIII. Gravitational lensing. *Astron. Astrophys.* **2020**, *641*, A8. [CrossRef]
81. Rosenberg, E.; Gratton, S.; Efstathiou, G. CMB power spectra and cosmological parameters from Planck PR4 with CamSpec. *arXiv* **2022**, arXiv:2205.10869.
82. Addison, G.E.; Huang, Y.; Watts, D.J.; Bennett, C.L.; Halpern, M.; Hinshaw, G.; Weiland, J.L. Quantifying discordance in the 2015 Planck CMB spectrum. *Astrophys. J.* **2016**, *818*, 132. [CrossRef]
83. Di Valentino, E.; Bridle, S. Exploring the Tension between Current Cosmic Microwave Background and Cosmic Shear Data. *Symmetry* **2018**, *10*, 585. [CrossRef]
84. Di Valentino, E.; Melchiorri, A.; Silk, J. Cosmological constraints in extended parameter space from the Planck 2018 Legacy release. *J. Cosmol. Astropart. Phys.* **2020**, *1*, 013. [CrossRef]
85. Aghanim, N. et al. [Planck]. Planck 2018 results. V. CMB power spectra and likelihoods. *Astron. Astrophys.* **2020**, *641*, A5. [CrossRef]
86. Di Valentino, E.; Melchiorri, A.; Silk, J. Planck evidence for a closed Universe and a possible crisis for cosmology. *Nat. Astron.* **2019**, *4*, 196–203. [CrossRef]
87. Efstathiou, G. Is the low CMB quadrupole a signature of spatial curvature? *Mon. Not. R. Astron. Soc.* **2003**, *343*, L95. [CrossRef]
88. Efstathiou, G.; Gratton, S. The evidence for a spatially flat Universe. *Mon. Not. R. Astron. Soc.* **2020**, *496*, L91–L95. [CrossRef]
89. Handley, W. Curvature tension: Evidence for a closed Universe. *Phys. Rev. D* **2021**, *103*, L041301. [CrossRef]
90. Vagnozzi, S.; Di Valentino, E.; Gariazzo, S.; Melchiorri, A.; Mena, O.; Silk, J. The galaxy power spectrum take on spatial curvature and cosmic concordance. *Phys. Dark Univ.* **2021**, *33*, 100851. [CrossRef]

91. Anselmi, S.; Carney, M.F.; Giblin, J.T.; Kumar, S.; Mertens, J.B.; Dwyer, M.O.; Starkman, G.D.; Tian, C. What is flat ΛCDM, and may we choose it? *arXiv* **2022**, arXiv:2207.06547.
92. Di Valentino, E.; Melchiorri, A.; Silk, J. Investigating Cosmic Discordance. *Astrophys. J. Lett.* **2021**, *908*, L9. [CrossRef]
93. Gonzalez, J.E.; Benetti, M.; von Marttens, R.; Alcaniz, J. Testing the consistency between cosmological data: The impact of spatial curvature and the dark energy EoS. *J. Cosmol. Astropart. Phys.* **2021**, *11*, 060. [CrossRef]
94. Handley, W.; Lemos, P. Quantifying the global parameter tensions between ACT, SPT and Planck. *Phys. Rev. D* **2021**, *103*, 063529. [CrossRef]
95. Forconi, M.; Giarè, W.; Di Valentino, E.; Melchiorri, A. Cosmological constraints on slow roll inflation: An update. *Phys. Rev. D* **2021**, *104*, 103528. [CrossRef]
96. Poulin, V.; Smith, T.L.; Bartlett, A. Dark energy at early times and ACT data: A larger Hubble constant without late-time priors. *Phys. Rev. D* **2021**, *104*, 123550. [CrossRef]
97. Hill, J.C.; Calabrese, E.; Aiola, S.; Battaglia, N.; Bolliet, B.; Choi, S.K.; Devlin, M.J.; Duivenvoorden, A.J.; Dunkley, J.; Ferraro, S.; et al. The Atacama Cosmology Telescope: Constraints on Pre-Recombination Early Dark Energy. *arXiv* **2021**, arXiv:2109.04451.
98. Di Valentino, E.; Melchiorri, A. Neutrino Mass Bounds in the Era of Tension Cosmology. *Astrophys. J. Lett.* **2022**, *931*, L18. [CrossRef]